Structural Analysis Modeling of Unbonded Prestressing in Prestressed Concrete Containments

R. A. Dameron[1)], P. P. Chang[1)], and M. F. Hessheimer[2)]

1) David Evans and Associates, San Diego, CA, USA
2) Sandia National Laboratories, Albuquerque, NM, USA[a]

ABSTRACT

Containment structural analysts need to develop models that represent the geometry, structural details and material properties which are 'important' to the response regime being analyzed and to the goals of the analysis. With continuing advances in computational tools, the trend has been to model containments with more elements, more detail, and more comprehensiveness than ever before. The focus of this paper is on the evolution and lessons learned related to modeling of unbonded prestressing tendons (or their effects) in prestressed concrete containments.

This paper presents an overview of the modeling options used by the authors or by others during many years of containment integrity research at Sandia National Laboratories. The paper then discusses the strengths, limitations, and challenges of various modeling methods, and prioritizes the levels of modeling sophistication in context with the goals of the analysis, and uncertainties of existing input and validation data. A number of scale model tests and analytical efforts are cited to show trends within the industry and lessons learned.

The paper also presents results of finite element analyses of a "ring model" (slice through a typical containment cylinder), comparing different prestress tendon modeling strategies. These range from simulation as embedded rebar with and without stress variation due to friction, to discrete tendon models with explicit representation of friction using contact surfaces.

INTRODUCTION

As with other aspects of containment modeling, approaches to modeling tendons have increased in sophistication and complexity over the last two decades. Various analysts world-wide [1], [2], [3] have taken different steps to simulate the effects of (1) angular and wobble friction, (2) anchorage setting losses, (3) differences between wire behavior and strand behavior, e.g. "wrapping angle", (4) non-strain-compatibility between tendons and concrete, (5) other losses such as creep, shrinkage, and tendon relaxation, and (6) nonlinear material behavior (with increasing pressure). Friction, strain compatibility, and temperature phenomena can change from that of normal "service" conditions to "overpressure" or accident conditions. But there remain real limits on what the state-of-the-art in material models can simulate and, generally, limits on the experimental data that exist for interpreting and verifying complex modeling representations. Reviewing various analysis work over the last decade has provided the following observations.

Friction phenomena are generally not modeled, but friction losses are sometimes included by manually assigning different prestressing levels to different locations. A few analysts have simulated initial condition friction by using friction-tie elements. This works satisfactorily for containment response analysis at low pressures (typically, between zero and the design pressure), but as described later in this paper, may not reliably predict tendon stress redistribution at high pressure (pressures well into the nonlinear response range for the tendons and rebar). Anchor set losses have generally not been considered even though these losses have been found to influence containment behavior predictions at low pressures. Wrapping angle effects are sometimes considered, but require accurate stress-strain testing of the tendons to do so. The choice between modeling concrete-tendon strain compatibility versus modeling tendon sliding has been made by roughly 50% of the analysts in references reviewed; conclusions on the effectiveness of this assumption are described later in this paper. Losses due to creep, shrinkage, and tendon relaxation are generally considered by using standard design equations prior to assigning initial stresses to the tendons, and this appears to be adequate for most analysis applications. Finally, for analyses aimed at predicting overpressure capacity, 100% of analysts use some form of plasticity model to represent material nonlinearity.

A number of scale model tests of prestressed concrete containment vessel and component models have been conducted. Table 1 lists some of the major tests and includes a brief comparison of the results.

---

[a] *Sandia is a multi program laboratory operated buy Sandia Corporation, a Lockheed Martin Company, for the U.S. Department of Energy's National Nuclear Security Administration under Contract Number DE-AC04-94AL85000.*

INFORMATION FROM NUPEC/NRC 1:4 SCALE PCCV MODEL AND OTHER TESTS

The Nuclear Power Engineering Corporation (NUPEC) of Japan and the U.S. Nuclear Regulatory Commission (NRC), Office of Nuclear Regulatory Research, co-sponsored and jointly funded a Cooperative Containment Research Program at Sandia National Laboratories (SNL) in Albuquerque, New Mexico. As a part of the program, a prestressed concrete containment vessel (PCCV) model was subjected to a series of overpressurization tests at SNL beginning in July 2000 and culminating in a functional failure mode or Limit State Test (LST) in September 2000 and a Structural Failure Mode Test (SFMT) in November 2001 [4]. The PCCV model, uniformly scaled at 1:4, is representative of the containment structure of an actual Pressurized Water Reactor (PWR) plant in Japan. The objectives of the tests were to obtain measurement data for the structural response of the model to pressure loading beyond design basis accident in order to validate numerical modeling, to find pressure capacity of the model, and to observe its failure mechanisms. Since the unique feature of the PCCV model, compared to previous large scale containment model tests, was the prestressing system, particular attention was paid to the design, construction and instrumentation of this component of the model.

Table 1. Summary of Results of Experiments for Prestressed Concrete Containment Models

Test	Scale	Shape	R/t	Pressure Ratio	Global Strain at Failure	Liner Material	Remarks
Indian Model	1:12	(CANDU)	20	1.9	-	1mm steel liner	Liner tearing and leakage esp. around penetration
Polish Model	1:10	(CANDU)	20	1.9	-	1mm steel liner	Liner tearing and leakage esp. around penetration
Canadian Model	1:14	Gentilly-2: 4-buttress w/ ring buttress	12.6	8.6	-	none (hydrostatic)	Vertical and hoop tendon rupture.
Sizewell-B (CEGB)	1:10	Sizewell-B	8.6	2.4	-	Rubber bladder (hydrostatic)	Basemat bending failure
NUPEC/NRC PCCV (SNL)	1:4	Large, dry PWR: 2-buttress cylinder w/ hemispherical dome	16.5	0.39* 3.6	-- 1.4%	SGV 410	LST: Liner tear/leakage SFMT: Tendon rupture and through-wall rupture

*Design pressure (MPa).

The arrangement of the prestressing tendons in the 1:4-scale PCCV model was identical to the prototype (Figure 1). The prestressing consisted of 180º 'hairpin tendons (vertical) and 360º (hoop) tendons, alternately anchored in opposing vertical buttresses. The tendons each consisted of three seven-wire-strands, inserted in galvanized metal ducts, then tensioned.

Figure 1. Arrangement of Tendons in PCCV Model

Prestressing levels for the model tendons were selected so that the net anchor forces (considering all losses due to anchor seating, elastic deformation, creep, shrinkage and relaxation) at the time of the Limit State Test matched those expected in the prototype after 40 years of service. One further adjustment was made by increasing the vertical tendon stress level to account for the additional gravity load in the prototype, which is lost in geometric scaling. Eight instrumented tendons and load cells at the ends of 1/6th of the model tendons were monitored continuously during prestressing. Load cells were installed at both ends of selected hoop tendons and meridional tendons to measure anchor forces during and after prestressing and during pressure testing. The tendon force distribution was determined by measuring strain at discrete points of individual wires comprising the tendon. Unfortunately over half of the strain gages installed on the tendons were damaged during prestressing operations. But enough survived to provide useful data on the tendon response during prestressing and pressurization tests. Since all model sensors were scanned during and after prestressing, the overall response of the model to prestressing forces as well as ambient thermal response and time dependent effects was also recorded.

Due to space limitations, this paper only focuses on hoop tendon behavior. The response of a typical tendon is illustrated by examining a hoop tendon (H53) at the mid-height of the cylinder wall. The force profiles for tendon H53 during the pneumatic Limit State Test of the PCCV model are shown in Figure 2. This figure also compares the measured force distribution in the tendon during and after tensioning with the design assumption. The data for the horizontal tendons generally confirms the assumed design force distribution.

There was inadequate data during the LST to assume the shape of the hoop tendon force profile between the surviving measurement positions, so only the force at the measurement locations are shown. There was enough data to suggest, however, that the tendon force distribution tends to become more uniform, with the largest increase in strain occurring near the mid-point of the tendon, where the initial prestressing force was the smallest. This is probably due to a combination of local yielding and slipping as the tendons maintain equilibrium and follow local deformation of the cylinder wall. Comparing the differential strain at the midpoint of the tendons to the hoop strain calculated from the wall displacement at that location (see Figure 2), indicates the tendon strain is greater than that expected if the tendon did not slip relative to the wall. After unloading, however, the initial tendon force profile (at the start of the LST) is almost completely recovered, which implies that redistribution that occurs during the LST is mostly elastic. This observation reinforces the conclusion that the change in tendon forces is partly due to slippage and partly due to local yielding.

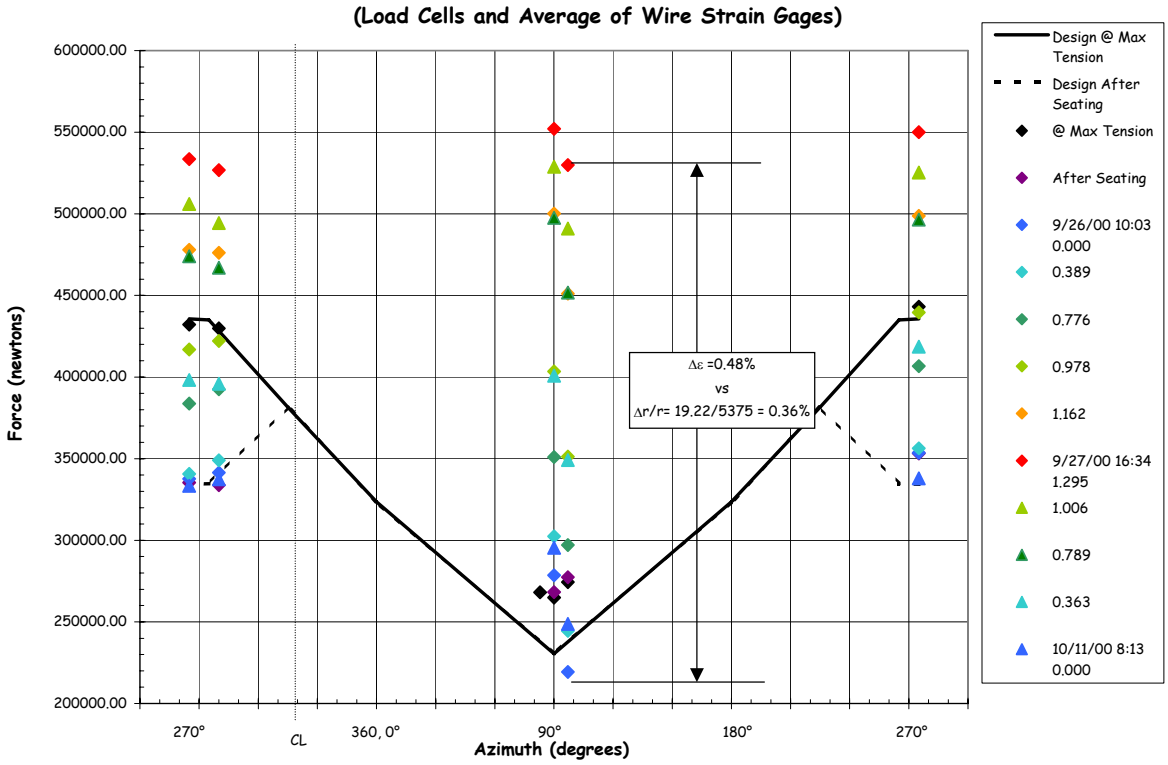

Figure 2 H53 Tendon Force Distribution, El. 6579

All the tendon load cells and strain gages which survived the LST were still functioning and all were monitored during the SFMT. Several load cells and tendon strain gages failed after filling the PCCV with water or early during the SFMT, presumably, due to water leaking from the model damaging the gage or shorting out the wiring. Near the end of the SFMT, sudden decreases in load were observed for several hoop tendon load cells, and these were interpreted as individual strand wires breaking. The acoustic monitoring system also gave evidence of tendon wire and strand breaks. After reaching peak pressure, all load cell readings dropped sharply as the tendons and the model ruptured. The hoop tendon strains at maximum pressure were on the order of 1.4% to 1.5%, 0.4% due to prestressing plus 1.0 to 1.1% due to the pressure load. While there may be some local strain concentrations which were not captured by the strain gages, the limiting tendon strain is substantially less than the ultimate strain obtained from laboratory tests of straight tendon samples, typically on the order of 4% for the tendon and up to 7% for individual strands. Further, none of the model tendons ruptured at anchors where tendon failures might be expected, but all ruptured where the deformation of the model was greatest, approximately Azimuth 6º.

As SFMT pressure increased, generalized yielding of the model and tendons occurred. Force profiles indicated that the tendon force became more uniform along the length, approaching a limiting value of approximately 600kN (135 kips). This provided more evidence to consider the issue of whether the tendon force equilibrates by slipping or if the friction is high enough to effectively bond the tendon to the concrete. The result of calculating the local, displacement-based strain in the wall and, assuming the tendon behaves as if it is bonded, adding it to the initial prestressing strains and computing the force profile from these strains, is shown in Figure 3. The results seem to compare favorably and reinforce the idea that the tendons behave as if they were bonded when the model reached high pressure.

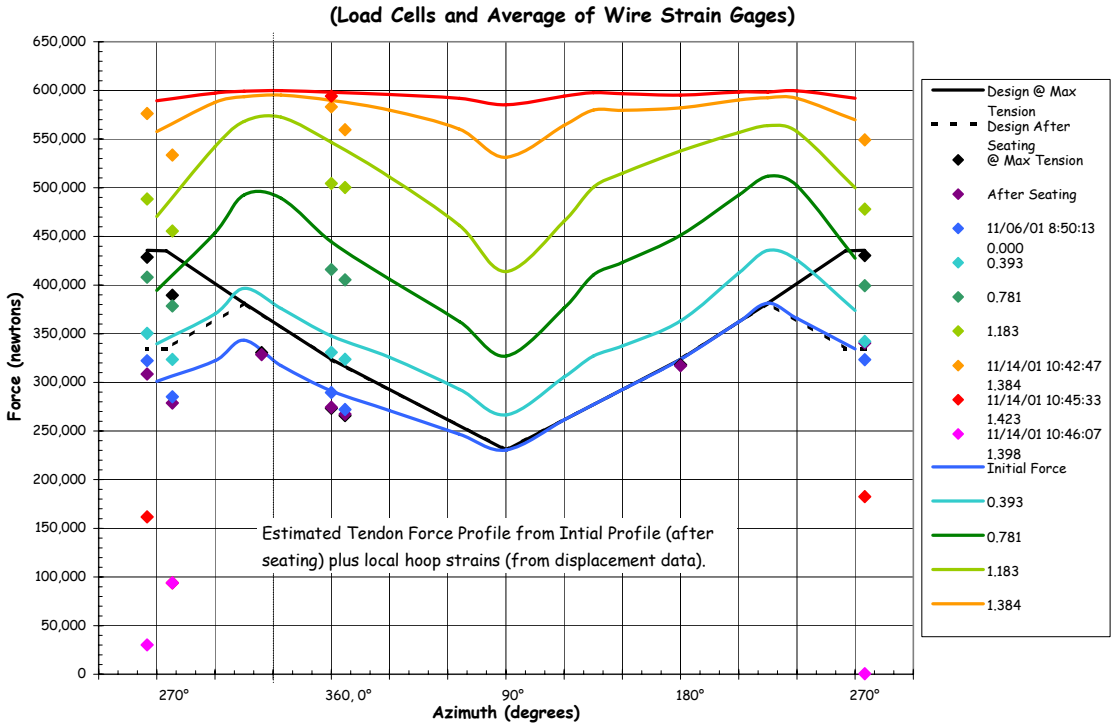

Figure 3 SFMT – Tendon H35 Computed and Measured Force Distribution

Similar conclusions were reached from the combined experimental and analytical evidence documented in a 1:10-scale model of a prestressed concrete containment vessel by the CEGB in the United Kingdom, 1989. This model of the Sizewell-B NPP containment utilized seven-wire strands in plastic sheaths to represent the vertical hairpin and hoop tendons. Sandia and ANATECH provided test and analysis support to the test, all of which is summarized in [5]. Failure of this test model occurred when excessive bending of the basemat slab led to rounding of the underside of the basemat, model tilting and potential instability, spalling of basemat under-surface concrete, and termination of the test. Concentrations of wall flexure, tendon strain measurements, and comparisons with analysis predictions using bonded and unbonded tendon assumptions all supported a conclusion that these tendons behaved in a bonded manner during the high pressure testing.

ANALYTICAL MODELING

As described in [1] and [6], detailed analytical studies were performed by ANATECH and by David Evans and Associates, Inc. under contract with Sandia for the 1:4 Scale PCCV Model. The final pretest prediction analyses were performed with a global axisymmetric, a semi-global three-dimensional cylinder midheight (3DCM) model, and local models of the Equipment Hatch (E/H), Personnel Airlock (A/L), and Mainsteam (M/S) penetrations. The ABAQUS general purpose finite element program [7] and the ANACAP-U concrete and steel constitutive modeling modules [8] were used for the analysis. Tendons and their prestressing were modeled to replicate expected tendon stress-strain behavior and friction effects. Concrete cracking was simulated with the "smeared crack" approach, where cracking is introduced at the finite element integration points. Rebar was always modeled with ABAQUS rebar subelements, which reside within the "parent" concrete element, and therefore, are required to have strain compatibility with the concrete. However, the rebar stress-strain law is different than the concrete and is represented by a J-2 plasticity model. The tendons were modeled in various ways for the different models, depending on the level of detail. In some cases, the tendons were modeled with rebar subelements, and in other cases, modeled individually with beam elements in which the tendon elements were allowed to slide relative to the concrete. In these cases, friction was represented in various ways. Tendon friction modeling was studied in detail in this work. The analytical failure predictions consisted of identification of liner tearing locations, all occurring near the midheight of the cylinder near penetrations, weld seams, and other liner discontinuities.

Beginning in 2003, a new approach to modeling tendon friction was investigated. To begin studying the technique, the final 3DCM model was reduced to a ring model representing an infinitely long cylinder as shown in Figure 4. Similar to the semi-global 3DCM model the concrete was modeled with brick elements, the liner with shell elements and the rebar was included as rebar sub-elements. Tendons were modeled with a truss element and, initially, friction truss-ties to adjacent concrete nodes. With the old approach, the friction truss-ties are oriented at the appropriate angle of friction between the tendon nodes and the concrete nodes, and this transmits friction according to the standard design assumption. For the 1:4 Scale Model, ancillary tendon friction tests were conducted which showed an angular friction coefficient, μ, of 0.21.

$$\text{Standard Angular Friction Loss Calculation: } P_x = P_o e^{-\mu\alpha} \quad (1)$$

where P_x = prestressing force at point x, P_o = prestressing force at stressing end, μ = coefficient of angular friction, and α = sum of angular deviations (in radians) over the distance x. For most full scale PCCVs, 0.11 is used. (This makes sense when considering that full scale ducts are greased and the curvatures are much smaller than in the scale model. As a point of comparison, it is also interesting to note that other prestressed structures, such as bridges, use similar values for m. For standard galvanized steel ducts, AASHTO [9] requires $\mu = 0.20$, and for "PT-PLUS^{TM} plastic ducts, $\mu = 0.14$.)

Once a baseline ring model had been developed and tested, the friction truss-ties were removed and replaced with a sliding contact surface, coefficient of friction equal to 0.21. In the original 3DCM analysis the stress in the tendon was applied through an initial stress in elastic elements, external to the concrete mesh, at the end of each tendon. Anchor set losses in the tendons were simulated by adjusting the orientation of the friction truss-ties near the end of each tendon. This was a tedious modeling process, and though aided by the use of mesh generation programs, it was still labor intensive to conduct tendon friction sensitivity studies. Further, the friction truss-ties required the use of "small displacement" theory so that the tendon friction would be oriented correctly regardless of the movement of tendon nodes relative to concrete nodes. Because the orientation of the truss-ties does not change, the shape of the tendon stress profile is "locked in," and this was found to have significant effects on the analysis at intermediate pressures (pressures in the range of 1.5 Pd to 3 Pd). Because the truss-ties are eliminated in the contact surface model, modeling different frictions is far easier, and the "small displacement theory" was no longer required. The tendons could be stressed in two steps, similar to the way stressing operations occur in the field. The tendons are stressed first to the full design stress and then the stressing is reduced to simulate anchor set losses. This second step allows the ends of the tendon to slip relative to the concrete. By using large displacement theory the tendon stress profile matched the design stress profile quite closely. The tendon stress distribution for the old method and for the new contact surface model at various applied pressures is shown in Figure 5.

Comparing the contact surface method to the friction truss tie method, the initial stress profiles of both methods are similar. But the behavior of the two models differs substantially once pressure is applied (up to pressures of approximately $2P_d$, where P_d is the design pressure), as shown in the radial displacement pattern plots of Figures 6 and 7. Comparison to the measured radial displacements shows that the contact surface model provides good prediction of 3D behavior of the cylinder, even at intermediate pressures, whereas the friction tie model displacement predictions showed too much displacement at the buttresses at intermediate pressures. The contact surface model has now been used to study sensitivity to other friction parameters, such as differences in angular friction, and differences in anchor set. These differences were shown to have significant influence on containment response (different radial deflections at different azimuths) for low

pressures (P = 0 through $2P_d$,), but little influence at high pressures ($P>3P_d$) after significant rebar and tendon yielding have occurred.

CONCLUSIONS

Efforts in previous containment testing programs to collect force distribution data on unbonded tendons have been generally unsuccessful. Sandia made a significant effort for the PCCV Model to investigate, develop and demonstrate the feasibility of measuring the tendon strains within the constraints of the program schedule and budget. The focus of this effort was on adapting or modifying 'off-the-shelf' components for this task. The biggest challenge for the instrumentation was surviving the harsh mechanical environment imposed on the sensors (and lead wires) during the prestressing operations. A number of promising non-contact sensors were investigated for the PCCV test to avoid this problem, but they were ultimately abandoned due to cost or difficulty with integrating them into the model. While the results were not completely satisfactory, due to the high mortality rate (>50%) experienced by the strain gages, a significant amount of data was collected, unique for prestressed concrete structures, and the feasibility of measuring the variation in tendon strain, and indirectly force, along the length was demonstrated. If future tests are planned, improvements in these sensors or new types of sensors, might make them an attractive alternative to the methods employed in the PCCV test, and should be considered.

Based on analyzing the test measurement data and on structural analysis, the following conclusions have been reached:

- The initial force distribution in the hoop tendons, i.e. during prestressing, appear to corroborate conventional design models for friction and anchor set.
- The tendons appear to 'slip' relative to the concrete wall during tensioning, and during early pressurization. As pressurization continues, the force distribution becomes nearly uniform. This appears to be due to a combination of tendon yielding, which naturally spreads zones of uniform stress along the tendon, and continued tendon slippage.
- But at high pressures near failure, the tendon strain distributions imply some attributes of tendon bonding; for example, the tendons which ruptured in the SFMT, ruptured at the azimuth with the largest displacements, rather than near the anchorages where conventional methods would predict failure to occur.
- A description of steps, guidelines, and lessons learned from the analytical studies of the 1:4 scale PCCV and other studies is provided in [5]. Among the lessons learned are those related to modeling tendons. It was found that the best modeling methods are, in descending order of preference, 1) a sliding contact friction surface between the tendons and the concrete, 2) pre-set friction ties applied in one direction during prestressing and then added in the other direction during pressurization, and 3) using a bonded tendon assumption with an "average" initial stress after friction and other losses.

REFERENCES

1. Dameron, R. A., et al. 2000. *Pretest Analysis of a 1:4-Scale Prestressed Concrete Containment Vessel Model*, NUREG/CR-6685, SAND2000-2093. Albuquerque, NM: Sandia National Laboratories.
2. EDF/IPSN, "Prestress Loss in NPP Containments," Joint WANO/OECD – NEA Workshop, Civaux NPP, Poitiers France, 1997, NEA/CSNI/R(97)9.
3. Nuclear Energy Agency Committee on the Safety of Nuclear Installations, "Finite Element Analysis of Aging Reinforced and Prestressed Concrete Structures in Nuclear Plants," July, 2002, NEA/CSNI/R(2002)13.
4. Hessheimer, M. F., Klamerus, E. W., Rightley, G. S., Lambert, L. D. and Dameron, R. A., "*Overpressurization Test of a 1:4-Scale Prestressed Concrete Containment Vessel Model*", NUREG/CR-6810, SAND2003-0840P, Sandia National Laboratories, Albuquerque NM. March, 2003.
5. Hessheimer, M.F. and Dameron, R. A., "Containment Integrity Research at Sandia National Laboratories – An Overview," Sandia National Laboratories Report, NUREG/CR-6906, SAND2006-2274P, July, 2006.
6. Dameron, R.A., et al. 2002. Posttest Analysis of the NUPEC/Sandia 1:4 Scale Prestressed Concrete Containment Vessel. NUREG/CR-6809, SAND2003-0839P, Albuquerque, NM: Sandia National Laboratories.
7. ABAQUS Users Manual, Version 5.8, 1998. Providence, RI: Hibbitt, Karlsson & Sorensen, Inc.
8. ANACAP-U User's Manual, Version 2.5, 1997. San Diego, CA: ANATECH Corp.
9. AASHTO LRFD "Bridge Design Specifications," American Association of State Highway and Transportation Officials, 2004.

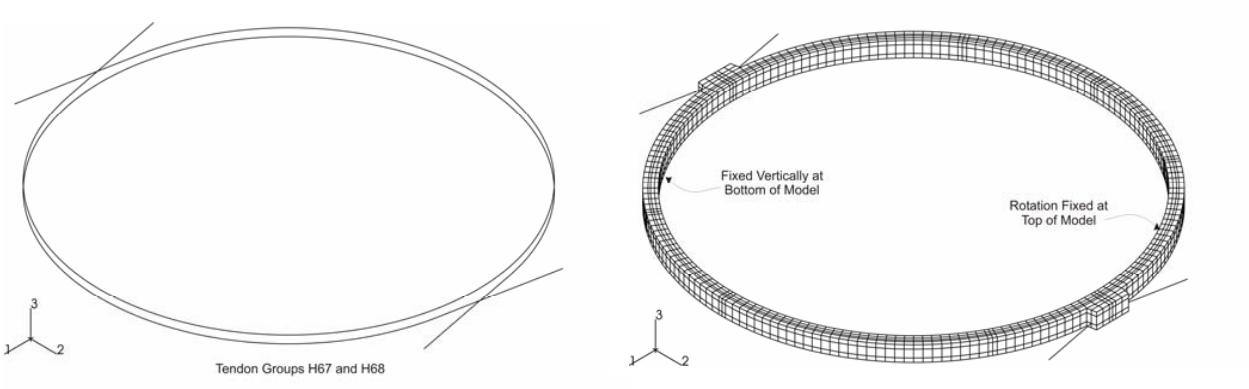

Figure 4 Ring Model Tendons and Boundary Conditions

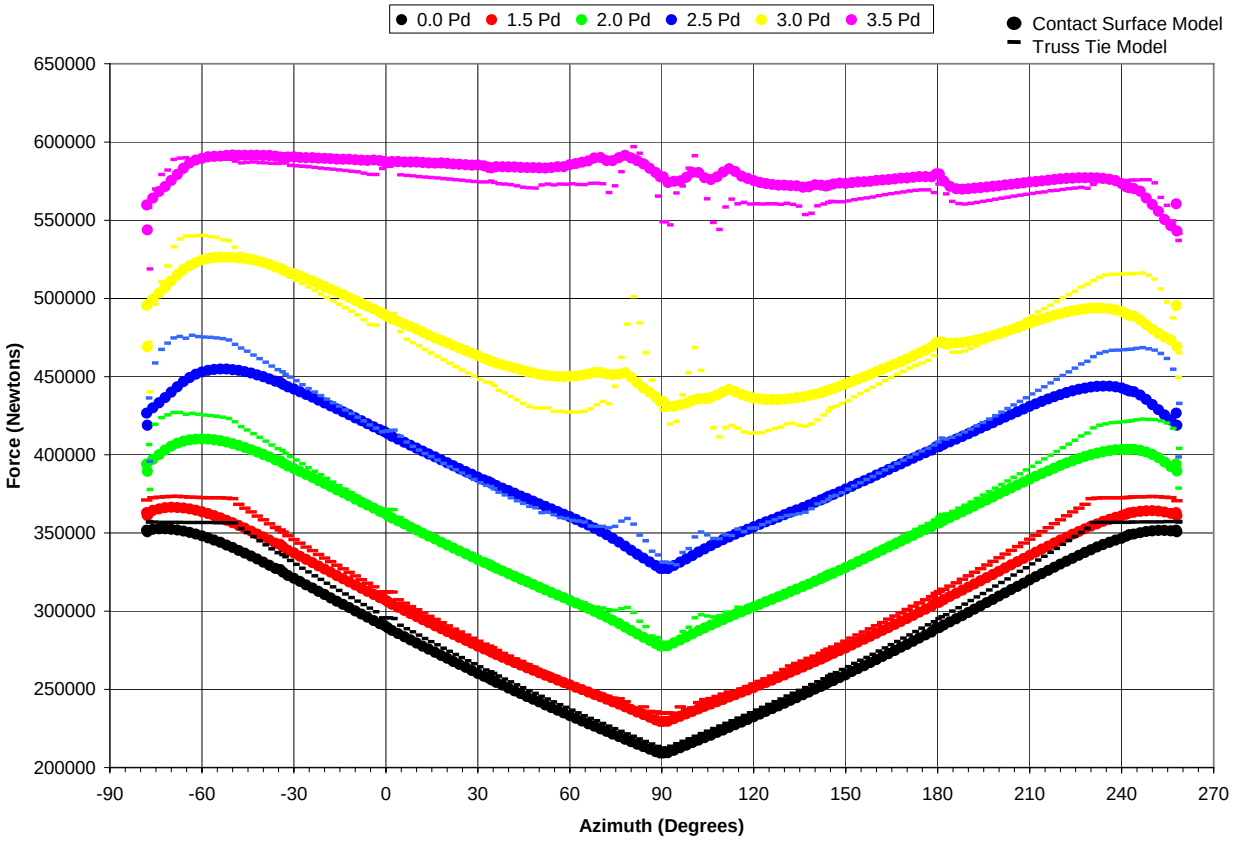

Figure 5 Comparison of Tendon Force Distributions for Two Tendon Friction Modeling Strategies

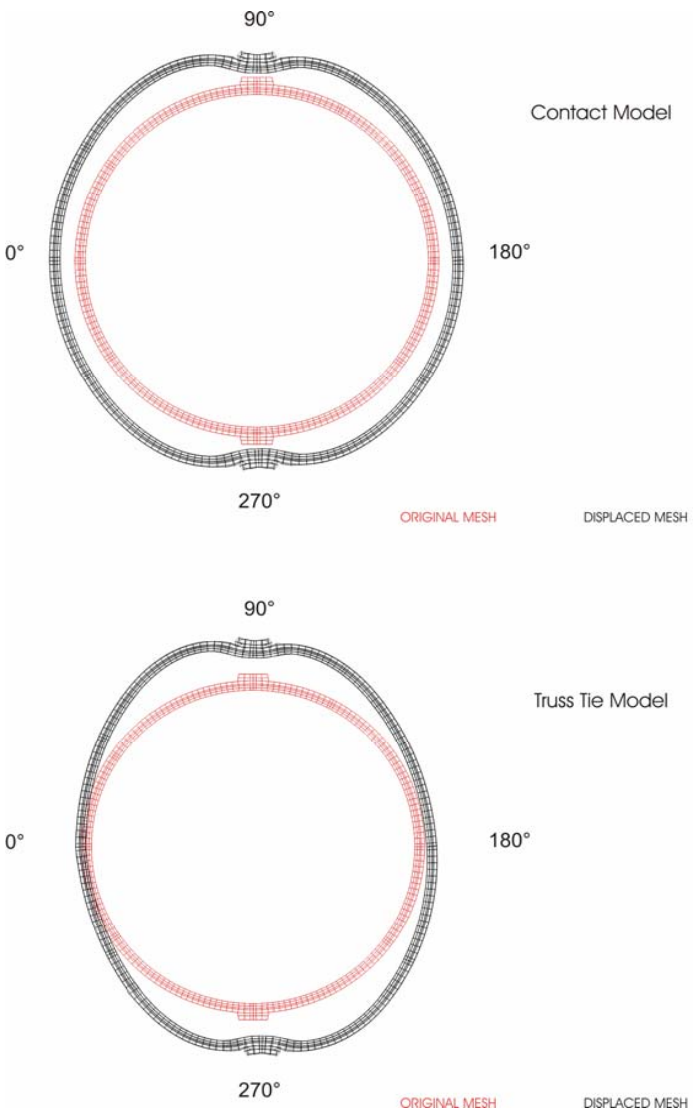

Figure 6 Comparison of Deformed Shapes (displ. x 200) Using Tendon Friction Truss Ties vs. the Contact Surface Model at P=2.0Pd

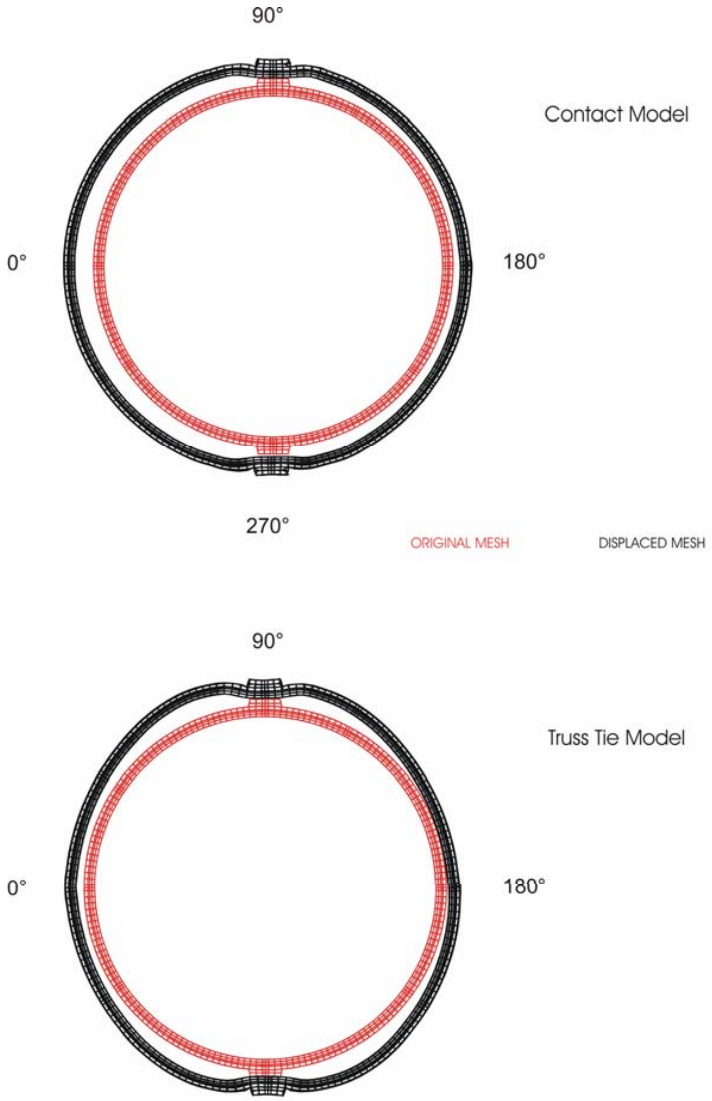

Figure 7 Comparison of Deformed Shapes (displ. x 20) Using Tendon Friction Truss Ties vs. the contact Surface Model at P=3.5P